Sensors and Actuators B 238 (2017) 565–577

Contents lists available at ScienceDirect

Sensors and Actuators B: Chemical

journal homepage: www.elsevier.com/locate/snb

Rhodamine based "turn–on" molecular switch FRET–sensor for cadmium and sulfide ions and live cell imaging study

M. Maniyazagan[a], R. Mariadasse[b], J. Jeyakanthan[b], N.K. Lokanath[d], S. Naveen[d], K. Premkumar[c], P. Muthuraja[a], P. Manisankar[a], T. Stalin[a,*]

[a] Department of Industrial Chemistry, School of Chemical Sciences, Alagappa University, Karaikudi-03, Tamil Nadu, India
[b] Structural Biology and Bio-Computing Lab, Department of Bioinformatics, Alagappa University, Karaikudi-04, Tamil Nadu, India
[c] Cancer Genetics and Nanomedicine Laboratory, Department of Biomedical Science, Bharathidasan University, Tiruchirappalli, Tamil Nadu, India
[d] Dept. of Studies in Physics, University of Mysore, Mansagangotri, Mysore 570006, India

ARTICLE INFO

Article history:
Received 13 May 2016
Received in revised form 14 July 2016
Accepted 20 July 2016
Available online 21 July 2016

Keywords:
Rhodamine
Fluorescence sensor
Förster resonance energy transfer
Metal ions
HeLa cells

ABSTRACT

A novel fluorescent chemosensor based on a rhodamine derivative (RBD4) was designed, synthesized, and used as a selective Cd^{2+} ion sensor. The structure of the fluorescence sensor (RBD4) is confirmed through single crystal X-ray study. On the basis of the Förster resonance energy transfer mechanism between rhodamine and pyridine conjugated dyad, a new colorimetric as well as fluorescence probe was synthesized for the selective detection of Cd^{2+}. This sensor shows high selectivity towards Cd^{2+} ions in the presence of other competing metal ions. On the basis of thorough experimental and theoretical findings, the additions of Cd^{2+} ions to the solution of RBD4 helps to generate a new fluorescence peak at 590 nm due to the selective binding of Cd^{2+} ions with RBD4 in a 1: 1 ratio with a binding constant (K) of $4.2524 \times 10^4\ M^{-1}$. The detection limit of RBD4 for Cd^{2+} was 1.025×10^{-8} M, which presented a pronounced sensitivity towards Cd^{2+}. The *in situ* generated RBD4–Cd^{2+} complex is able to selectively sense S^{2-} over other anions based on the displacement approach, given a remarkable recovery of fluorescence and UV–vis absorption spectra. The fluorescence sensor has also exhibited very good results in HeLa Cells imaging under physiological pH.

1. Introduction

Heavy-metal pollution has become hazardous to the environment and human health [1]. A Cadmium ion (Cd^{2+}), a redundant element for life, is extensively used in batteries and fertilizers, resulting in the extensive contamination of it in air, water, and soil [2]. It is not only a severe environmental hazard but also can be a severe health threats to humans [3,4]. A cadmium ion has been recognized as a highly toxic heavy metal ion and is enlisted by the U.S. Environmental Protection Agency, Disease Registry, and Agency for Toxic Substances as one of the superior pollutants [5]. This poisonous cadmium ion may enter in human body or living beings through uptake of contaminated water, food or inhalation of smoke (cigarette smoke). The exposure (may be long- or short-term) to Cd^{2+} may cause renal dysfunction, mutations, calcium metabolism disorders, as well as an increased incidence of cancers [6].

In addition, it can accumulate in the human body for >10 years [7–11]. The extensive use of cadmium metal in agriculture and industrial fields lead to water and soil contamination. Cadmium ions contamination is mainly derived from phosphate fertilizers, Ni-Cd batteries, metal alloys, ceramic enamels, paint pigments and natural factors like erosion, volcanic eruption and abrasion [12–14]. The intake of cadmium ions by the cells has showed an adverse effect in molecular mechanism, cellular functions and causes so many acute health diseases like kidney cancer, lung cancer, prostate cancers and renal cancer. Smoking and inhalation of cadmium-containing dust represent additional sources of cadmium uptake in humans. Cadmium ions accumulation is involved in reproductive, neurological, cardiovascular, and developmental disorders [15–17]. Even the fertility of the soil is affected primarily with cadmium ions contamination which leads to the poor growth of corps.

Consequently, there are great needs for a highly selective and sensitive method to quantify and recognize cadmium ions in environmental samples as well as in the living cells as the cellular uptake and carcinogenic mechanisms of cadmium ions are still poorly understood. In this view, the fluorescence spectroscopy is

* Corresponding author.
E-mail address: drstalin76@gmail.com (T. Stalin).

http://dx.doi.org/10.1016/j.snb.2016.07.102
0925-4005/

a promising and powerful tool for sensing and imaging metal ions, and the development of fluorescence sensors has much interest increasing attention of the researchers in the recent years [18–23].

The development of highly selective and efficient signalling systems to detect various chemically and biologically relevant species has attained significant interest [24,25]. Recently, great efforts have been made to develop artificial optical receptors for highly selective and sensitive anion recognition for their important roles in industrial, biological, and environmental processes. As one of the members, sulfide is broadly used in different fields, for instance, conversion into sulfur and sulfuric acid, cosmetic manufacturing and dyes, production of wood pulp, etc. [26]. As a consequence, the sulfide anion can be widely found in water not only owing to industrial processes but also thanks to microbial reduction of sulfate by anaerobic bacteria or formed from the sulfur-containing amino acids in meat proteins. Sulfide can irritate mucous membranes and even cause unconsciousness and respiratory paralysis [27,28]. Once sulfide protonated to produce HS^- or H_2S, sulfide will become even more toxic. At a low concentration, H_2S can produce personal distress, while at a higher concentration; it can result in loss of consciousness, permanent brain damage, or even death through asphyxiation [29]. Therefore, it is important to develop a rapid and sensitive method for immediate sulfide monitoring in aqueous media and in biological systems.

In recent years, Förster resonance energy transfer (FRET) is a widely used sensing mechanism for the design of fluorescence colorimetric probes. This nonradiative process involves the energy transfer between a pair of fluorophores that acts as energy donor and acceptor linked together through a nonconjugated spacer. The basic requirements to show high FRET efficiency are a substantial overlap between the emission of the donor moiety and absorption bands of the acceptor moiety and an appropriate distance between the donor and acceptor (~10–100 Å) as the energy transfer occurs through space [30,31].

Rhodamine based fluorescent probes, its colourless and non-fluorescent nature in its spiro ring-closed form and, in contrast, the pink-red coloured and strong fluorescence in the ring-opened form, rhodamine dye was extremely popular in the field of probe design across the past decade [32–41]. Rhodamine dye acts as a good acceptor fluorophore in a system exhibiting FRET mechanism. The characteristic emission of a rhodamine-based dye in the spiro ring-closed form is inhibited, and the FRET dyad shows only the emission of the donor. Consequently, the FRET process of the system is prohibited, whereas, after reaction/complexation with relevant analyte, the spiro ring of the rhodamine dye opens, which gives a strong emission, consequently activating the FRET process "ON". Taking such advantage of the rhodamine dye, to date, a number of the rhodamine-based FRET sensors have been reported for different types of analytes [42–48].

For the past one decade, the corresponding author has largely been involved in studying the molecular spectroscopic properties [49–53] of the interactions of various organic molecules with β–cyclodextrin. In addition the development of a chemosensor (Host–guest complexes) probe capable of recognizing behaviour is very challenging [54–56]. This molecule (Rhodamine B) shows intramolecular charge transfer emission in the excited singlet state. This stimulated us to carry out a study on synthesis, crystal structure of rhodamine derivative as a fluorescence sensor for Cd^{2+} and S^{2-}. In this paper, we report a novel fluorescent sensor, RBD4, based on rhodamine B and 2-Pyridinecarboxaldehyde as the receptor. The receptor can combine Cd^{2+} to form complex RBD–Cd^{2+}, which displays high sensitivity and selectivity for S^{2-} over other possible competitive anions on the basis of forming CdS. The 1:1 complexation RBD4–Cd^{2+} was characterized by X-ray powder diffraction (XRD), Scanning Electron Microscopy (SEM), Energy-dispersive X-ray spectroscopy (EDX), Fourier transform infrared spectroscopy (FT–IR) and Job's plot. The photophysical properties and recognition behaviours of the chemosensor have been investigated in detail through UV–vis absorption spectra, fluorescence spectra, theoretical calculations, and fluorescence images in biological cells.

2. Experimental section

2.1. General information and materials

All of the materials for synthesis were purchased from commercial suppliers and used without further purification. The absorption spectra were recorded on a Schimadzu UV-PC-2401 UV–vis spectrophotometer using 10 mm path length quartz cuvettes in the range 300–800 nm wavelengths, while the fluorescence measurements were carried on a JASCO FP-8200 spectrofluorometer using 10 mm path length quartz cuvettes with a slit width of 5 nm at 298 K. FT–IR spectra were measured on a JASCO FTIR 4600 FT–IR spectrometer with 4 cm^{-1} resolution and 32 scanned between wave number 4000 cm^{-1} and 400 cm^{-1}. Samples were prepared KBr disks with 1 mg of complex in 100 mg of KBr. The mass spectra of RBD4 are recorded using Agilent Technologies 6520 Accurate mass spectrometer. NMR spectra were recorded on a Varian FT–400 MHz instrument. The chemical shifts were recorded in parts per million (ppm) on the scale. The following abbreviations are used to describe spin multiplicities in ^1H NMR spectra: s = singlet; d = doublet; t = triplet; m = multiplet.

2.2. Synthesis of the rhodamine b hydrazide

In 100 ml flask, rhodamine B (1.20 g, 2.5 mmol) was dissolved in 30 ml of ethanol, 3.0 ml of excess hydrazide hydrate (85%) was then added dropwise with vigorous stirring at room temperature. After the adding, the stirred mixture was heated to reflux in an air bath for 2 h. The solution changed from dark purple to light orange and became clear. Then the mixture was cooled and the solvent was removed under reduced pressure. 1 M HCl (about 50 ml) was added to the solid in the flasks to generate a clear red solution. After that 1 M NaOH (about 70 ml) was added slowly with stirring until the pH of the solution reached 9–10. The resulting precipitate was filtered and washed 3 times with 15 ml of water.

Yield: 79%, mp (°C): 191 ± 2, ^1H NMR ($CDCl_3$), δ (ppm): 1.16 (t, 12H, $NCH_2\underline{C}H_3$, J = 7.0 Hz), 3.33 (q, 8H, $N\underline{C}H_2CH_3$, J = 7.0 Hz), 3.64 (bs, 2H, NH_2), 6.32 (dd, 2H, Xanthene-H, J_1 = 9.0 Hz, J_2 = 2.4 Hz), 6.39(d, 2H, Xanthene-H, J = 2.4 Hz), 6.46 (d, 2H, Xanthene-H, J = 9.0 Hz), 7.11 (dd, 1H, Ar-H, J_1 = 5.4 Hz, J_2 = 3.3 Hz), 7.42 (d, 1H, Ar-H, J = 3.3 Hz), 7.44 (d, 1H, Ar-H, J = 3.3 Hz), 7.94 (dd, 1H, Ar-H, J_1 = 5.4 Hz, J_2 = 3.3 Hz). ^{13}C NMR ($CDCl_3$) δ (ppm): 12.8, 44.58, 66.11, 76.81, 77.23, 77.44, 77.66, 98.23, 104.83, 108.28, 123.19, 124.03, 128.28, 130.24, 132.70, 149.11, 151.75, 154.06 and 166.35. FT-IR spectra of rhodamine b hydrazide revealed that the peak at 1735 cm^{-1}, the characteristic frequency for the $C{=}O_{Amide}$ bond of the rhodamine unit. Strong stretching frequencies at 3500 and 1690 cm^{-1} were observed in the IR spectra of rhodamine B hydrazide due to N—H stretching of NH_2 (primary amine) and N—C=O (amide) stretching respectively. FT-IR (KBr) cm^{-1}: 3280, 3204 (νNH and νNH_2); 2923.38, 2810 (νCH); 1685.90 (νC=O); 1613.64, 1513.57 and 1496 (νAr = CH). ESI-Mass m/z calculated value for 457.1; experimental value is 457.2.

2.3. Synthesis of the sensor molecule (RBD4)

Rhodamine-B hydrazide (0.46 g, 1 mmol) was dissolved in 20 ml absolute ethanol. An excessive 2-Pyridinecarboxaldehyde (4 mmol) was added, and then mixture was refluxed in an air bath for 6 h. After that, the solution was cooled (concentrated to 10 ml) and allowed to stand at room temperature overnight. The precipitate

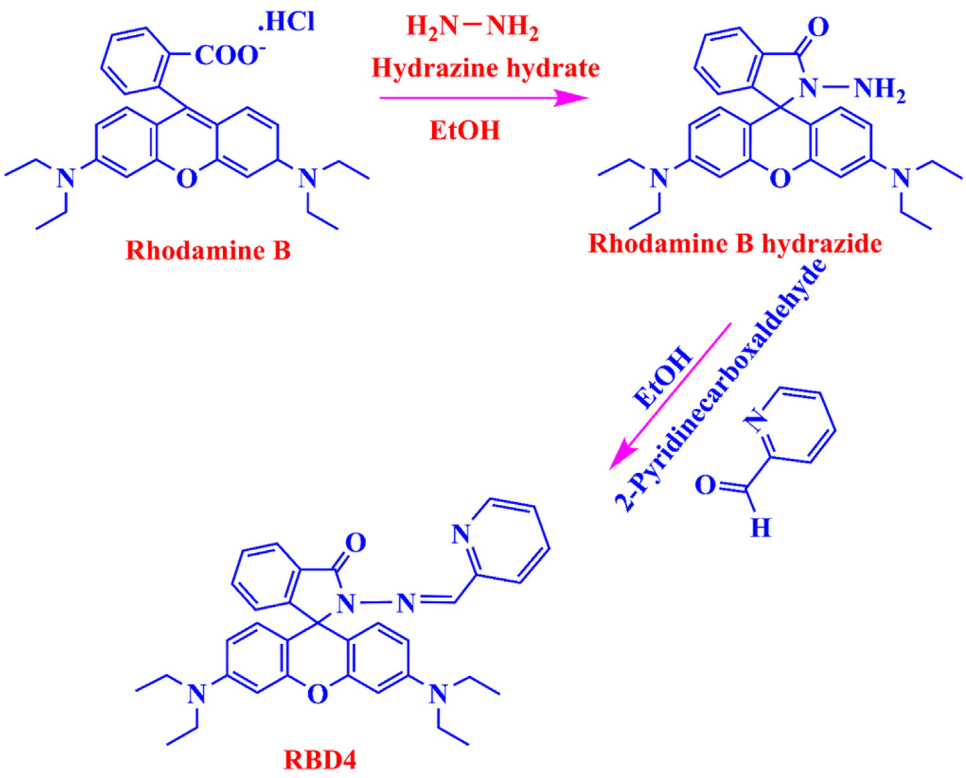

Scheme 1. Synthetic Scheme for probe RBD4.

which appeared next day was filtered and washed 3 times with 10 ml absolute ethanol. After drying under reduced pressure the reaction afforded 0.47 g of RBD4 (77%) as pink solid, mp (°C): 218 ± 2. ^{1}H NMR [$CDCl_3$), $SiMe_4$, J (Hz), δ (ppm)]: ^{1}H NMR (300 MHz, $CDCl_3$) δ 8.46 (d, J = 5.8 Hz, 1H), 8.00 (d, J = 8.1 Hz, 2H), 7.60 (t, J = 7.7 Hz, 1H), 7.52-7.40 (m, 2H), 7.12 (t, J = 6.5 Hz, 2H), 6.55 (d, J = 8.8 Hz, 2H), 6.45 (d, J = 2.4 Hz, 2H), 6.24 (dd, J = 8.8, 2.5 Hz, 2H), 3.31 (q, J = 7.1 Hz, 8H), 1.14 (t, J = 7.1 Hz, 12H). 13C NMR (75 MHz, CDCl3) δ 165.61 (s), 153.43 (s), 152.60 (s), 145.97 (s), 136.30 (s), 128.46 (s), 108.58 (s), 105.85 (s), 98.54 (s), 77.66 (s), 77.23 (s), 44.52 (s), 12.61 (s). ESI mass: calculated value for [($C_{34}H_{35}N_5O_2$)H] (M+H) is 545.67, experimental value 546.3.

2.4. UV–vis and fluorescence spectral studies

Stock solutions of various ions (1×10^{-3} mol l^{-1}) were prepared in deionized water. A stock solution of RBD4 (1×10^{-3} mol l^{-1}) was prepared in Acetonitrile (ACN). The solution of RBD4 was then diluted to 1×10^{-5} mol l^{-1} with ACN/HEPES buffer (2:8, v/v, 10 mM, pH 7.2). In titration experiments, each time a 1×10^{-3} mol l^{-1} solution of RBD4 (1×10^{-5} mol l^{-1}) was filled in a quartz optical cell of 1 cm optical path length, and the ion stock solutions were added into the quartz optical cell gradually by using a micropipette. Spectral data were recorded at 2 min after the addition of the ions. In selectivity experiments, the test samples were prepared by placing appropriate amounts of the anions/cations stock into 2 ml of solution of RBD4 (2×10^{-5} mol l^{-1}).

2.5. Computational details

All ground-state optimizations were carried out by DFT [57] calculations using Gaussian 09 [58–60]. All geometry optimizations were performed in the gas phase using the B3LYP functional. For C, H, N, and O the 6-31G* basis set was used, whereas for Cd^{2+} atoms the SDD effective core potential was used. Vibrational frequency calculations were done to verify the nature of the stationary points.

2.6. Cell culture and fluorescence imaging

HeLa, human cervical cancer cell line was procured from National Centre for Cell Sciences, Pune, India and cultured in DMEM (Himedia, India) containing 10% heat-inactivated fetal bovine serum (FBS), 100 units/ml penicillin G, 100 mg/ml streptomycin (Himedia, India), 2 mM glutamine (Gibco, USA), 25 mM HEPES, and 2 mM sodium bicarbonate under standard conditions in CO_2 incubator (Eppendorf – New Brunswick Galaxy incubator). 90% confluent cells were harvested and used for bioimaging studies.

HeLa cells were seeded in 6-well plates containing sterile circular cover-slips at a density of 3×10^5 cells/well. After 8 h, experimental cells were incubated with 20 μl of RBD4 for 1 h. After the incubation period, 20 μl the Cd^{2+} were added and incubated for another 4 h. After the treatment period, the experimental cells were rinsed with PBS to remove the remaining RBD4 and Cd^{2+} ions and visualized for fluorescence under Nikon Eclipse fluorescence microscope (Nikon, Inc., Melville, NY).

3. Results and discussion

Rhodamine B hydrazide was synthesized following a literature method [61] and characterized by ^{1}H NMR spectra, ^{13}C NMR spectra, ESI mass data, and FT-IR (Figs. S1–S4). It was then condensed with 2-Pyridinecarboxaldehyde in ethanol to form RBD4 in 77% yield (Scheme 1). The structure of compound RBD4 was confirmed by its spectroscopic, analytical data (^{1}H NMR, ^{13}CNMR, ESI–MS, Fig. S5–S7) and X-ray crystal structure analysis is shown in Fig. 1. Single crystals of RBD4 were obtained by slow evaporation of the acetonitrile solution (Tables S1).

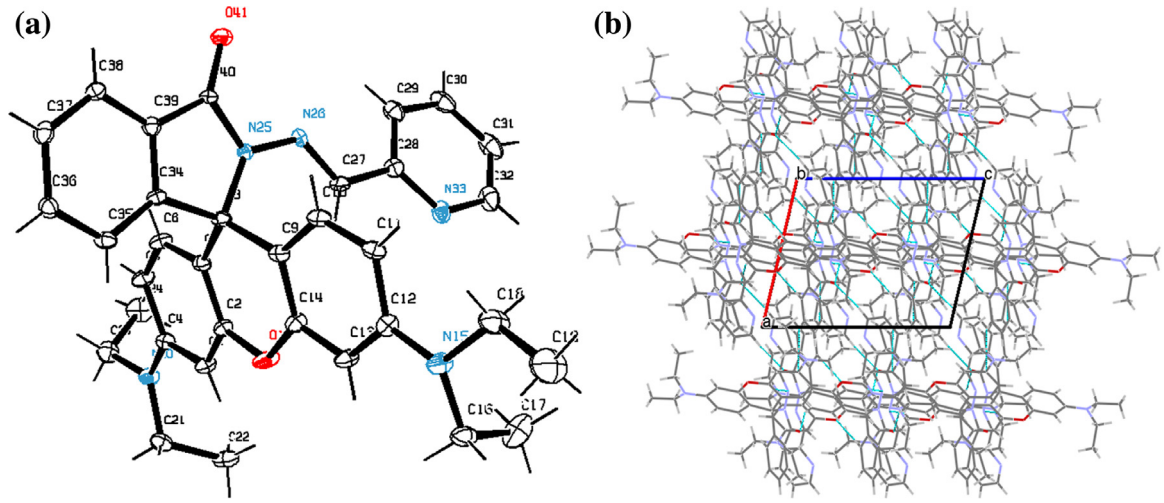

Fig. 1. X-ray crystal structure of RBD4 showing displacement ellipsoids drawn at the 30% probability level. Hydrogen atoms have been omitted for clarity (a). The crystal packing of RBD4. Intermolecular interactions have been omitted for clarity (b).

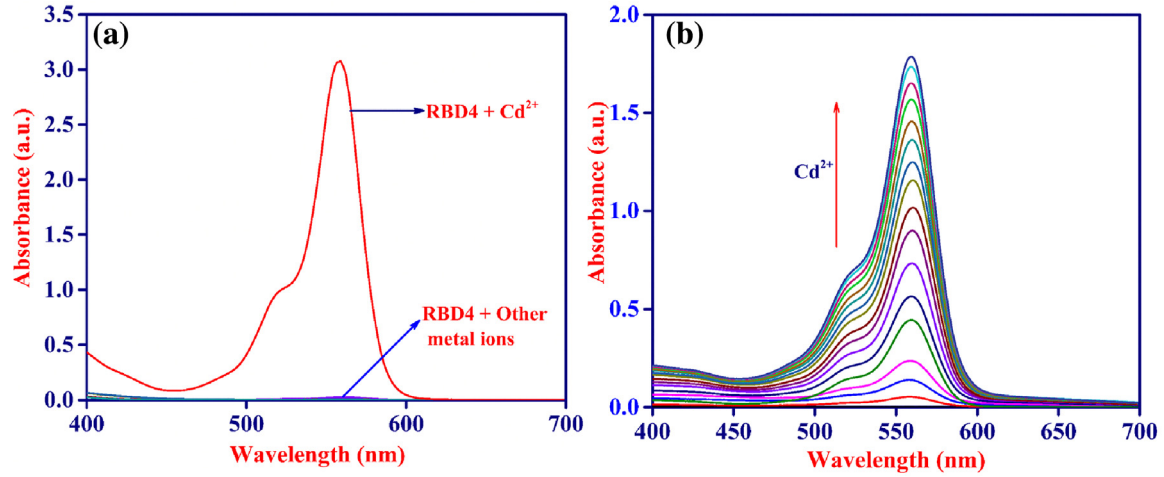

Fig. 2. UV–vis absorption spectra of probe RBD4 (100 μM) observed upon addition of 2 equiv of various cations in ACN/HEPES buffer (2:8, v/v, 10 mM, pH 7.2) (a). Absorption titration spectra of probe RBD4 (50 μM) with Cd^{2+} (0.0–1.0 equiv) in ACN/HEPES buffer (2:8, v/v, 10 mM, pH 7.2) (b).

3.1. UV–vis absorption spectroscopy study

We have carried out UV–vis titration experiments to understand the nature of binding of RBD4 to Cd^{2+}. The fluorescence sensor RBD4 (10 mM) in CH_3CN—H_2O (2: 8, v/v) buffered with 2-[4-(2-hydroxyethyl)piperazin- 1-yl]ethanesulfonic acid (HEPES), pH = 7.2 showed an absorption maximum at 308 nm, suggesting that the spirolactam ring of the rhodamine B unit preferred its ring-closed state under these conditions. The selectivity of RBD4 has been checked with different biologically important metal ions e.g., Na^+, K^+, Mg^{2+}, Hg^{2+}, Cu^{2+}, Pb^{2+}, Fe^{2+}, Fe^{3+}, Ca^{2+}, Ni^{2+}, Cd^{2+} and Al^{3+} in ACN/HEPES buffer (2:8, v/v, pH 7.2, 10 mM). A significant change in the UV–vis spectral pattern was observed only in the presence of Cd^{2+} among all the other metal ions used (Fig. 2a). Upon gradual addition of Cd^{2+} ions (0–100 mM) to chemosensor RBD4 (10 mM) in ACN/HEPES buffer (2:8, v/v, pH 7.2, 10 mM), a concomitant red shift in the spectral position at 560 nm was observed along with an increase in the absorption intensity. The emergence of the absorption band at 560 nm was due to the opening of the spirolactam ring of the rhodamine moiety along with a color change from colorless to deep magenta (Fig. 2b). The association constant [62] between RBD4 and the Cd^{2+} ion was calculated from the absorption titration result and was found to be $4.2524 \times 10^4\ M^{-1}$ at 25 °C (Fig. 3a). The peak values at 560 nm are plotted versus Cd^{2+} concentration (Fig. 3b), and a linear relationship is observed with a good regression coefficient ($R^2 = 0.9917$) in the concentration range from 0.5–50 μM with a detection limit is calculated to be 5.67×10^{-7} M which is far below the WHO acceptable limit in drinking water. Under the aforesaid conditions, addition of other metal ions did not cause any noticeable changes. The binding of Cd^{2+} ion induces opening of the spirolactam ring in RBD4 with an associated switch on UV–vis spectral response in the range 500–580 nm, which has a significant spectral overlap with the emission spectrum of the pyridine fragment, and this fact unlocks a plausible route for non-radiative transfer of excitation initiates an intramolecular FRET process. In the free fluorescent probe RBD4 the FRET pathway is totally suppressed, and only an emission maximum near 480 nm is observed when excited at 308 nm. Binding of the receptor to Cd^{2+} induces the FRET process to produce an intense rhodamine-based red emission; i.e., energy transfer from pyridine to xanthene is due to the ring-opening resulting in increase of overlap integral between pyridine and xanthene moiety (Scheme 2). The color of the solution was significantly changed from deep magenta to bright orange when illuminated with a hand-held UV lamp (Fig. 4). So it could easily be detected by the “naked-eye” without the need of any other instrumental assistance.

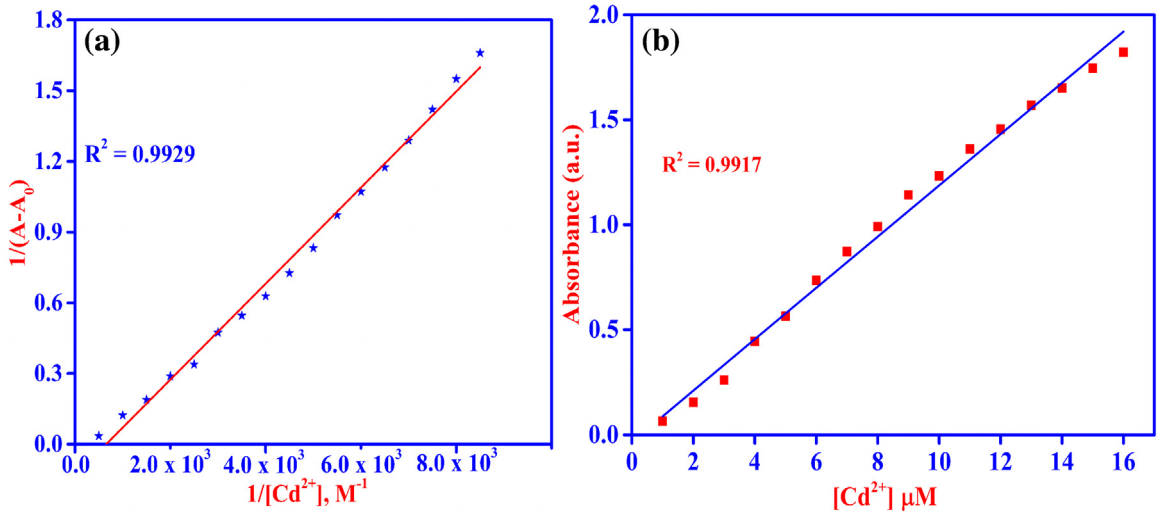

Fig. 3. Benesi–Hildebrand plot of chemosensor RBD4 (100 mM) in ACN/HEPES buffer (2:8, v/v, 10 mM, pH 7.2), absorbance at 560 nm (a). The linear responses with Cd^{2+} concentrations (b).

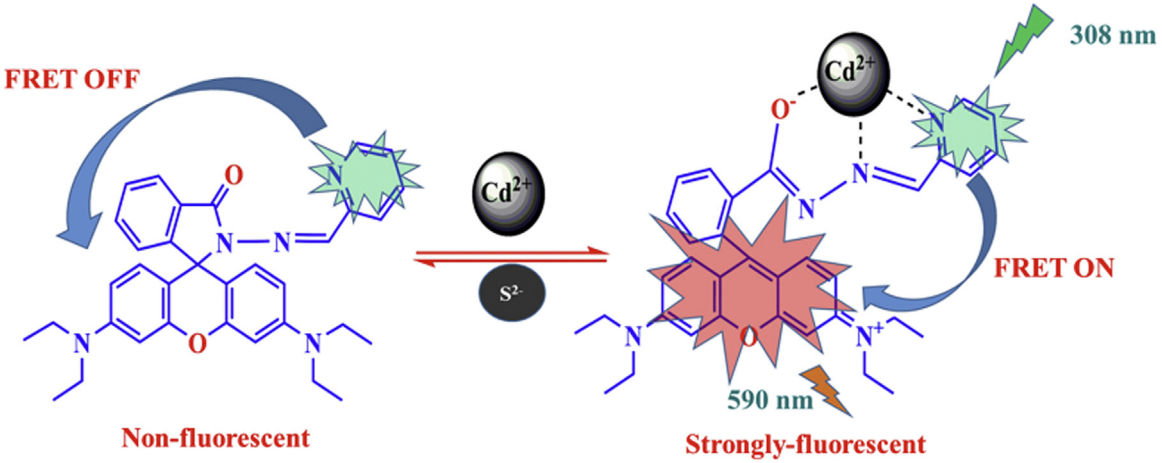

Scheme 2. Cd^{2+}-Induced FRET OFF → ON of the fluorescent probe RBD4.

3.2. Fluorescence spectroscopy study

The fluorescence spectrum of RBD4 (10 mM) in ACN/HEPES buffer (2:8, v/v, pH 7.2, 10 mM), exhibited an emission band at 590 nm when excited at 308 nm. Upon interaction with various metal ions e.g. Na^+, K^+, Mg^{2+}, Hg^{2+}, Cu^{2+}, Pb^{2+}, Fe^{2+}, Fe^{3+}, Ca^{2+}, Ni^{2+}, Cd^{2+} and Al^{3+} a much weaker spectral response was observed relative to Cd^{2+} ion at the same concentration (Fig. 5a). During sequential titration (0–100 mM of Cd^{2+}), the emission band peaked up at 590 nm which was attributed to delocalization in the xanthene moiety of the rhodamine and hence emission intensity was increased significantly (Fig. 5b). The observed fluorescence spetrum occurred due to the metal binding event induced an electronic rearrangement within the dye that opened the spirolactam and yielded a fully conjugated rhodamine dye. The solution showed an intense orange fluorescence, with an approximately 20-fold enhancement in the fluorescence intensity at 590 nm. This fact means that RBD4 could be used as an 'off–on' fluorescent chemosensor for Cd^{2+}. To investigate the recognition ability between RBD4 and the Cd^{2+} ion, Job's plot [63] experiment were carried out to determine the binding stoichiometry of the RBD4–Cd^{2+} complex. The absorption intensity varies through a maximum at a molar fraction of about 0.5 of Cd^{2+}, indicating a 1: 1 stoichiometry and this is the most possible case of binding of Cd^{2+} with RBD4 (Fig. 6).

To check the practical ability of fluorescence sensor RBD4 as a selective Cd^{2+} ion fluorescent chemosensor, we have carried out competitive experiments in the presence of Cd^{2+} ions mixed with other different metal ions (Na^+, K^+, Mg^{2+}, Hg^{2+}, Cu^{2+}, Pb^{2+}, Fe^{2+}, Fe^{3+}, Ca^{2+}, Ni^{2+} and Al^{3+}). The fluorescence response of the RBD4–Cd^{2+} system remains the same by comparison with or without the other metal ions (Fig. 7). These findings confirmed the highly selectivity, sensitivity and effective interaction of the fluorescent probe RBD4 with Cd^{2+}. For practical applications, the detection limit of RBD4 was also estimated. The fluorescence titration profile of RBD4 (10 mM) with Cd^{2+} demonstrated that the detection limit [64] of Cd^{2+} is 1.025×10^{-8} M which is far below the WHO acceptable limit (0.05 mg l^{-1} or 1.85 mM of Cd^{2+}) in drinking water (Fig. 8).

3.3. DFT study

The mode of binding of Cd^{2+} with the RBD4 was also studied by DFT calculations. The stoichiometry of the complexes was found to be 1:1 on the basis of absorption and emission spectroscopic studies, and this mononuclear complex was modelled by DFT calculations. The geometry optimization for free RBD4 and the

Fig. 4. Visual color change of probe RBD4 (100 μM) upon the addition of various metal ions (2 equivalents) in ACN/HEPES buffer (2:8, v/v, 10 mM, pH 7.2) (Top). Fluorescence color change of probe RBD4 (100 μM) upon the addition of various metal ions (2 equivalents) in ACN/HEPES buffer (2:8, v/v, 10 mM, pH 7.2) (Bottom).

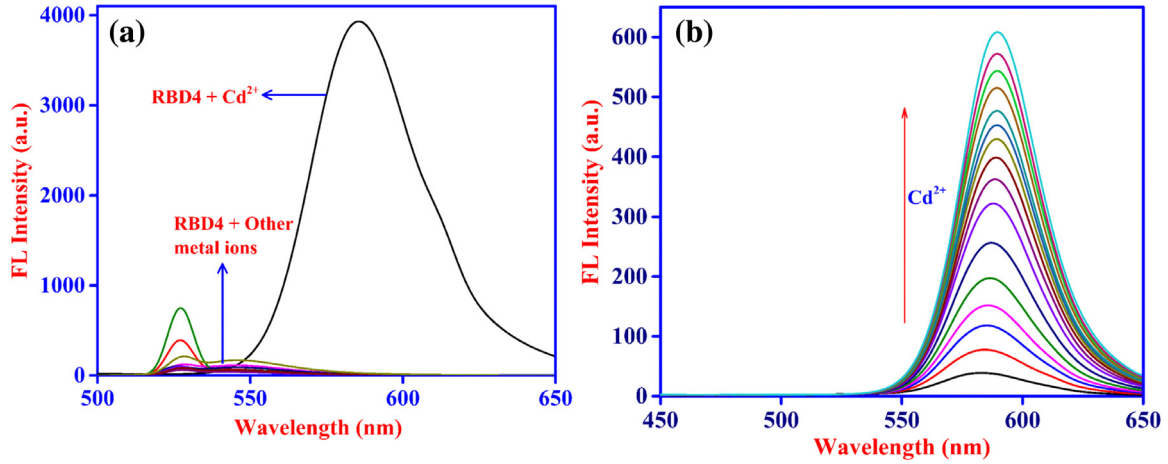

Fig. 5. Fluorescence spectra of probe RBD4 (100 μM) observed upon addition of 2 equiv of various cations in ACN/HEPES buffer (2:8, v/v, 10 mM, pH 7.2) (a). Fluorescence titration spectra of probe RBD4 (10 μM) with Cd^{2+} (0.0–1.0 equiv) in ACN/HEPES buffer (2:8, v/v, 10 mM, pH 7.2) (b) (λ_{ex} = 308 nm).

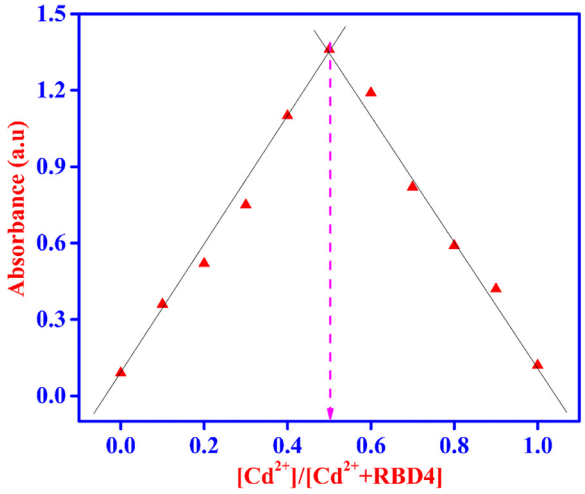

Fig. 6. Job's plot of probe RBD4 with Cd^{2+} ions in HEPES buffer indicating the formation of 1:1 complex.

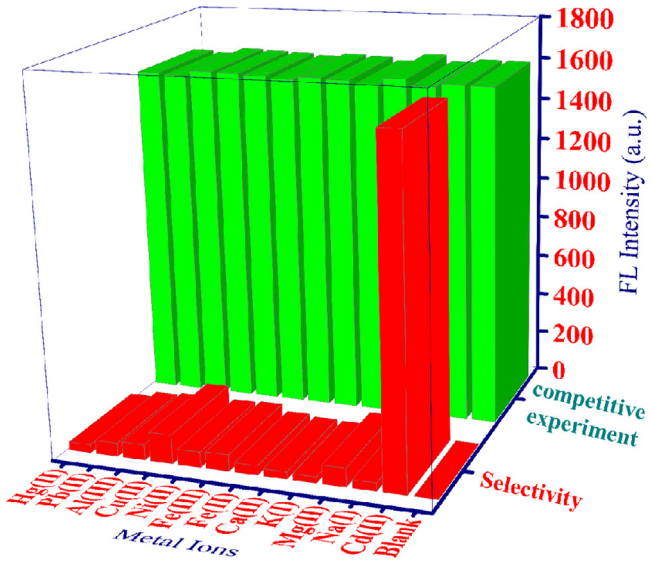

Fig. 7. Results of the competition experiments between Cd^{2+} and selected metal ions. The free RBD4 concentration was set at 10 μM, and the excitation was at 308 nm with a slit width of 5.0 nm. Solvent: ACN/HEPES buffer (2:8, v/v, 10 mM, pH 7.2).

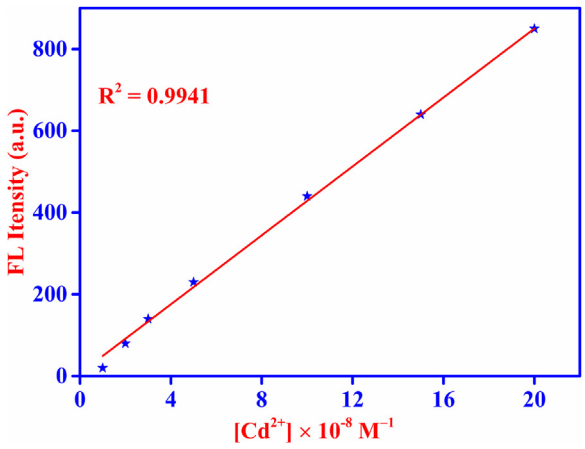

Fig. 8. Determination of the detection limit of Cd^{2+} by RBDB4 (10 mM) in ACN/HEPES buffer (2:8, v/v, 10 mM, pH 7.2), (λ_{ex} = 308 nm and λ_{em} = 590 nm).

corresponding complex (RBD4-Cd^{2+}) was done by DFT calculations. For RBD4-Cd^{2+} complex, ground-state-optimized structure of free RBD4 were generated and Cd^{2+} was kept well in the core of the amide O, pyridine N and imine N as donor atoms at a noninteracting distance. The HOMO–LUMO orbital energies and the spatial distributions for RBD4 and RBD4-Cd^{2+} were also determined (Fig. 9). The energy gaps between the HOMOs and LUMOs for receptor RBD4 were 49.6355 kcal mol^{-1}. Similarly, for complex (RBD4-Cd^{2+}) the energy gaps were found to be 21.6300 kcal mol^{-1} (Table S2). These results suggest that the binding mode of Cd^{2+} ion adopts NON coordination by bonding through the one nitrogen of the imine group, one nitrogen of the pyridine moiety and one oxygen atom of the carbonyl group, resulting in a nearly planar geometry around Cd^{2+}. The optimized structures of Cd^{2+} with receptors RBD4 shows that the individual low-energy complexation occurs between Cd^{2+} and NON atoms of the free RBD4. Hence, the interaction of NON with Cd^{2+} could change the HOMO–LUMO energy levels, and the electronic transitions.

3.4. Effect of pH and time course effect

To study the practical applicability, the effect of pH on the fluorescence response of the new chemosensor RBD4 towards Cd^{2+} has also been investigated. Experimental results show that for free RBD4, under acidic conditions (pH < 3), an obvious fluorescence off–on (Fig. 10a) situation appears due to the formation of the open-ring state because of the strong protonation, and it shows a fluorescence quenching effect upon addition of Cd^{2+}. In the pH range from 3 to 9, neither the color nor the fluorescence (excited at 560 nm) characteristics of rhodamine could be observed for RBD4, suggesting that the spirocyclic form was still preferred in this range. The time evolution of the receptor RBD4 in the presence of 5.0 equiv. of Cd^{2+} in ACN/HEPES buffer (2:8, v/v, pH 7.2, 10 mM) was investigated as shown in Fig. 10b. The probe RBD4 showed enhanced fluorescence in the high acidic pH but in stable in the rest pH range, whereas RBD4–Cd^{2+} did not showed in the basic range, due to the formation of $Cd(OH)_2$. This clearly indicates the applicability of the probe in sensing Cd^{2+} ion in physiological pH range. The recognition interaction gets almost completed just after the addition of 5 equiv. of Cd^{2+} and the fluorescence intensity remains almost the same up to 120 min.

3.5. Powder XRD analysis

XRD pattern of the RBD4 and RBD4–Cd^{2+} complexes are shown in Figs. 11. The XRD pattern of the metal complexes shows well defined crystalline peaks indicating that the samples were crystalline in phase. It can be easily seen that the pattern of the RBD4 differs from its RBD4–Cd^{2+} complex, which may be attributed to the formation of a complex between RBD4 and Cd^{2+}. The pattern reveals the successful formation of the above said complex, which is evident from the characteristic peaks. The obtained pattern was also matched with standard diffraction pattern, which shows an excellent agreement with the standard data. The XRD pattern for Cadmium(II) chloride matches with the standard pattern of Cd, JCPDS card number 05-0674.

3.6. SEM and EDX analysis

The SEM analysis was here carried out to check the surface morphology of the RBD4 (Fig. 12a) and RBD4–Cd^{2+} (Fig. 12b) complex. The micrograph of the RBD4 is represents that the obtained material has exhibited agglomerated crystalline nature. It is evident from the SEM study that the RBD4–Cd^{2+} complex shows the complex agglomerated crystalline nature. The difference in the shape of the RBD4 and RBD4-Cd^{2+} complex aggregates deposited was mainly

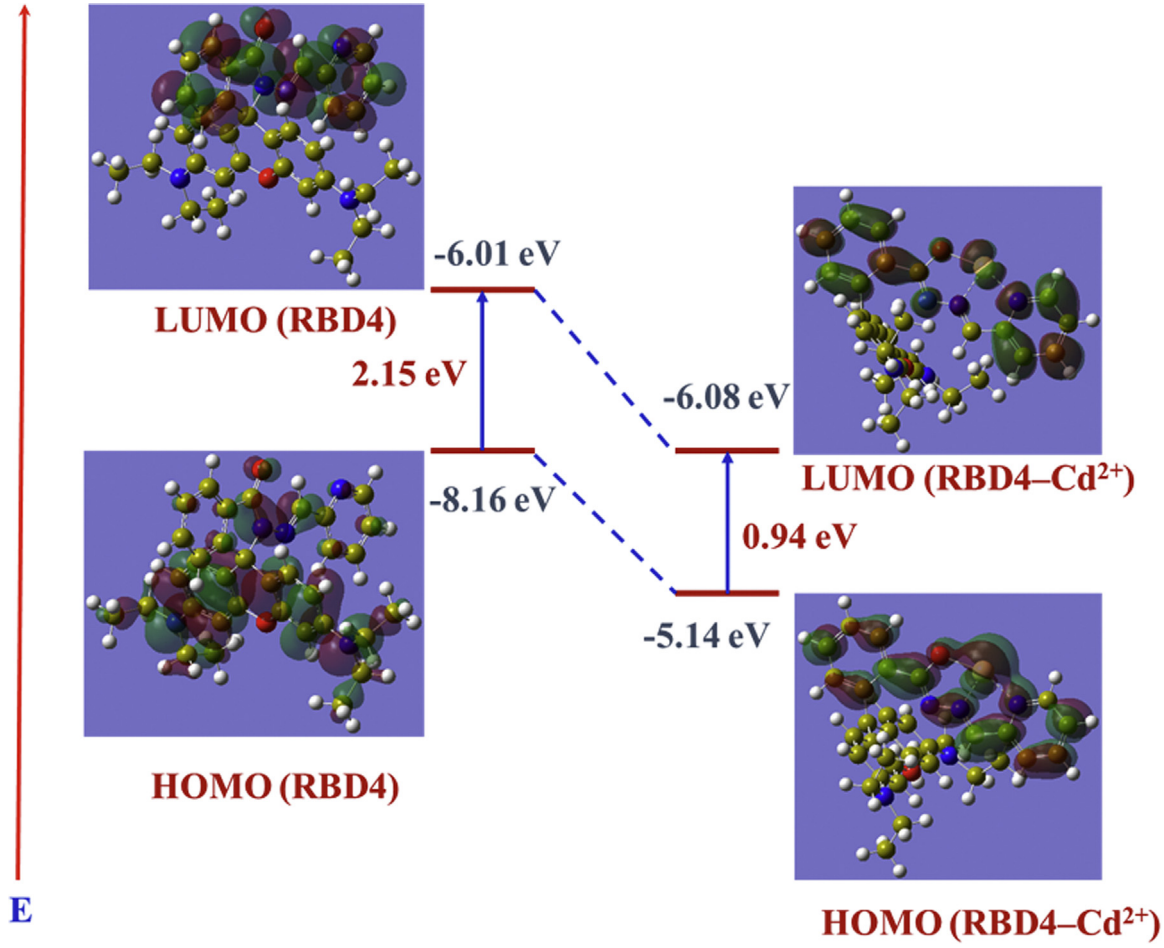

Fig. 9. Frontier molecular orbitals of RBD4 and RBD4–Cd^{2+}. HOMO and LUMO active representation of RBD4 (a & b). HOMO and LUMO active representation of RBD4-Cd^{2+} (c and d).

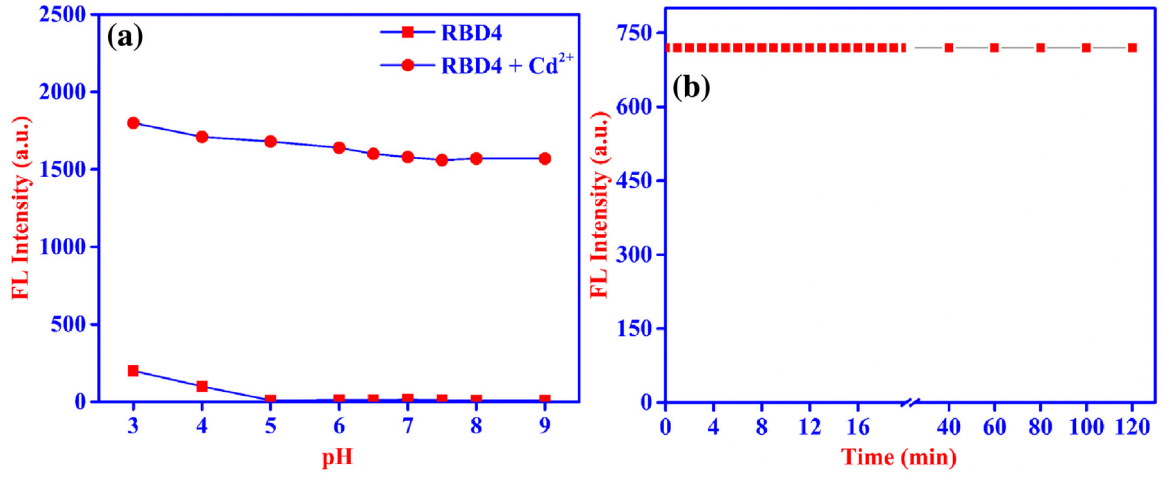

Fig. 10. Fluorescence intensity of RBD4 and RBD4–Cd^{2+} at various ranges of pH in ACN/HEPES buffer (2:8, v/v, 10 mM, pH 7.2) λ_{ex} = 308 nm (a). Time evolution for Cd^{2+} (b).

dependent on the Cd^{2+} ion. Fig. 12b and Fig. 12d shows the EDX spectrum of RBD4 and RBD4-Cd^{2+} complex. The EDX measurement confirmed the presence of Cd in the RBD4–Cd^{2+} complex.

3.7. FT–IR analysis

To confirm the nature of the complexation between RBD4 and RBD4–Cd^{2+}, the Fourier transform infrared (FT–IR) spectrum of RBD4 was recorded in the absence and presence of Cd^{2+} ion (Fig. S8). The spectrum presented rhodamine spirolactam amide carbonyl (C=O) stretching vibrations at 1689 cm^{-1} in addition to the xanthene–NH stretching vibrations at approximately 3440 and 2960 cm^{-1}. When 1 equiv. Cd^{2+} was added, the stretching vibrations of these functional groups changed, confirming the 1:1 stoichiometry for the RBD4–Cd^{2+} complex. In the free RBD4, the band at 1650 cm^{-1} is assigned to ν(C—N) frequency; after complex-

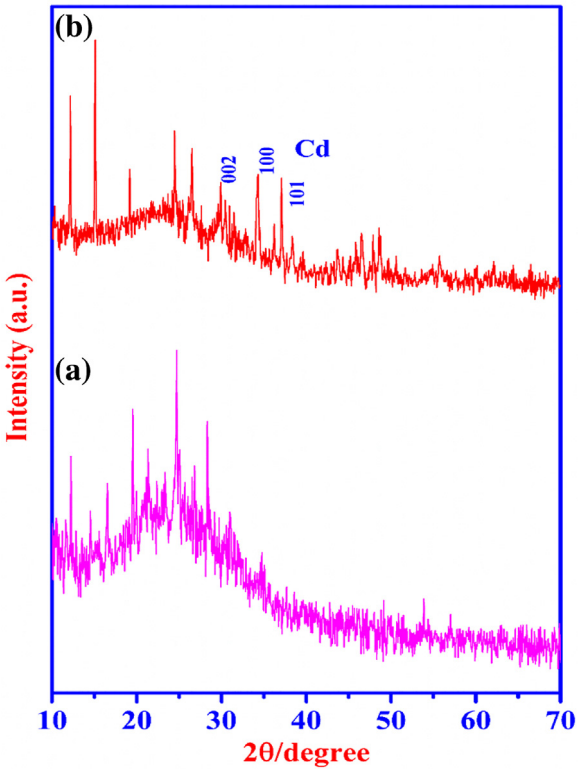

Fig. 11. X-ray diffraction pattern of RBD4 and RBD4–Cd^{2+} complex.

ation, this band is shifted to lower frequency. New bands appeared in the spectra of the complexes at 534–577 cm^{-1}, corresponding to O → M and 425–468 cm^{-1} due to the N → M vibrations which support the involvement of N and O atoms in complexation with metal ions under investigation.

3.8. Absorption studies of RBD4–Cd^{2+} complex in presence of S^{2-}

The aforesaid studies we can conclude that RBD4 selectively binds with Cd^{2+} to form RBD4–Cd^{2+} complex with significant change in its spectral studies. We have further studied the impact of different anions on the cleavage of this RBD4–Cd^{2+} complex and their effect on the reversibility of this complex to regenerate RBD4. The absorption properties of the RBD4–Cd^{2+}complex were studied in presence of different anions such as F^-, Cl^-, Br^-, I^-, CN^-, $H_2PO_4^-$, NO_3^-, ClO_3^-, ClO_4^-, HSO_3^-, SO_4^{2-}, PO_4^{3-}, and S^{2-}. The absorption spectral studies suggest that the regeneration of compound RBD4 is observed only by adding S^{2-} to the solution having RBD4–Cd^{2+}, whereas other anions did not show any remarkable changes in absorption spectra (Fig. 13a). The absorption spectral studies of the titration experiment was similar but in reverse direction to the spectra obtained with Cd^{2+} (Fig. 13b). This fact is evidence that fluorescent probe RBD4 is recovered from RBD4-Cd^{2+} in presence of S^{2-}. The interactions can be expressed in terms of hard and soft acids and bases (HSAB principle) the reactions are more favorable for hard-hard and soft-soft interactions than for a mix of hard and soft in the reactants (Cd^{2+} soft acid, S^{2-} soft base). Again, more electrons and larger size lead to softer behavior. Sulfide ion (S^{2-}) is softer than O2- because it has more electrons spread over a slightly larger volume, making S^{2-} more polarizable. Within a group, such comparisons are easy; as the electronic structure and size change, comparisons become more difficult but are still possible. Thus, S^{2-} is softer than Cl^-, which has the same electronic structure, because S^{2-} has a smaller nuclear charge and a slightly larger size. As a result, the negative charge is more available for polarization. Soft acids tend to react with soft bases and hard acids with hard bases, so the reaction (Cd^{2+}, S^{2-}) produces soft-soft combinations.

3.9. Fluorescence studies of RBD4–Cd^{2+} complex in presence of S^{2-}

The fluorescence spectral studies also shows that the emission spectra of the RBD4–Cd^{2+} complex returns to its original RBD4 state, selectively in presence of S^{2-} ions (Fig. 14a). In addition the fluorescence "ON–OFF" switching property of the fluorescent complex RBD4–Cd^{2+}, we have studied in fluorescence titration experiment. Fig. 14b shows that the intensity of the fluorescence emission maxima decreases with increasing concentration of S^{2-} ion, and on addition of near about 3 equiv. of S^{2-} anion both the intensity and the fluorescence spectrum closely match those of fluorescent probe RBD4. The aforesaid results suggested that the sensor RBD4 was recycled during the detection of S^{2-} ions.

The RBD4–Cd^{2+} spectral binding studies it was conform that the binding induced breakage of the spirolactam ring of RBD4 initiates the FRET pathway for efficient transfer of energy from pyridine moiety to the xanthene moiety. It is evident that the regeneration of RBD4 from RBD4–Cd^{2+} complex is possible in presence of S^{2-} ion then the removal of Cd^{2+} disturb the FRET process. Thus, increasing the concentration of S^{2-} ion to the RBD4–Cd^{2+} complex is in fluorescence emission spectrum which is equivalent to the fluorescence spectra of RBD4 (when excited at 308 nm). The aforesaid fact suggests strong evidence of the dissociation of RBD4–Cd^{2+} complex in presence of S^{2-} anions to restore the original structure of RBD4. The peak values at 590 nm are plotted versus Cd^{2+} concentration and a linear relationship is observed with a good regression coefficient (R2 = 0.9941) in the concentration range from 5×10^{-7} to 1.0×10^{-5} M The LOD value for sulfide ions for this method was found to be 1.2×10^{-7} M (Fig. S9). The intensities of the fluorescence were recorded within 15 min after sulfide anion addition and varied with time. As a result of this fact it may be concluded that the

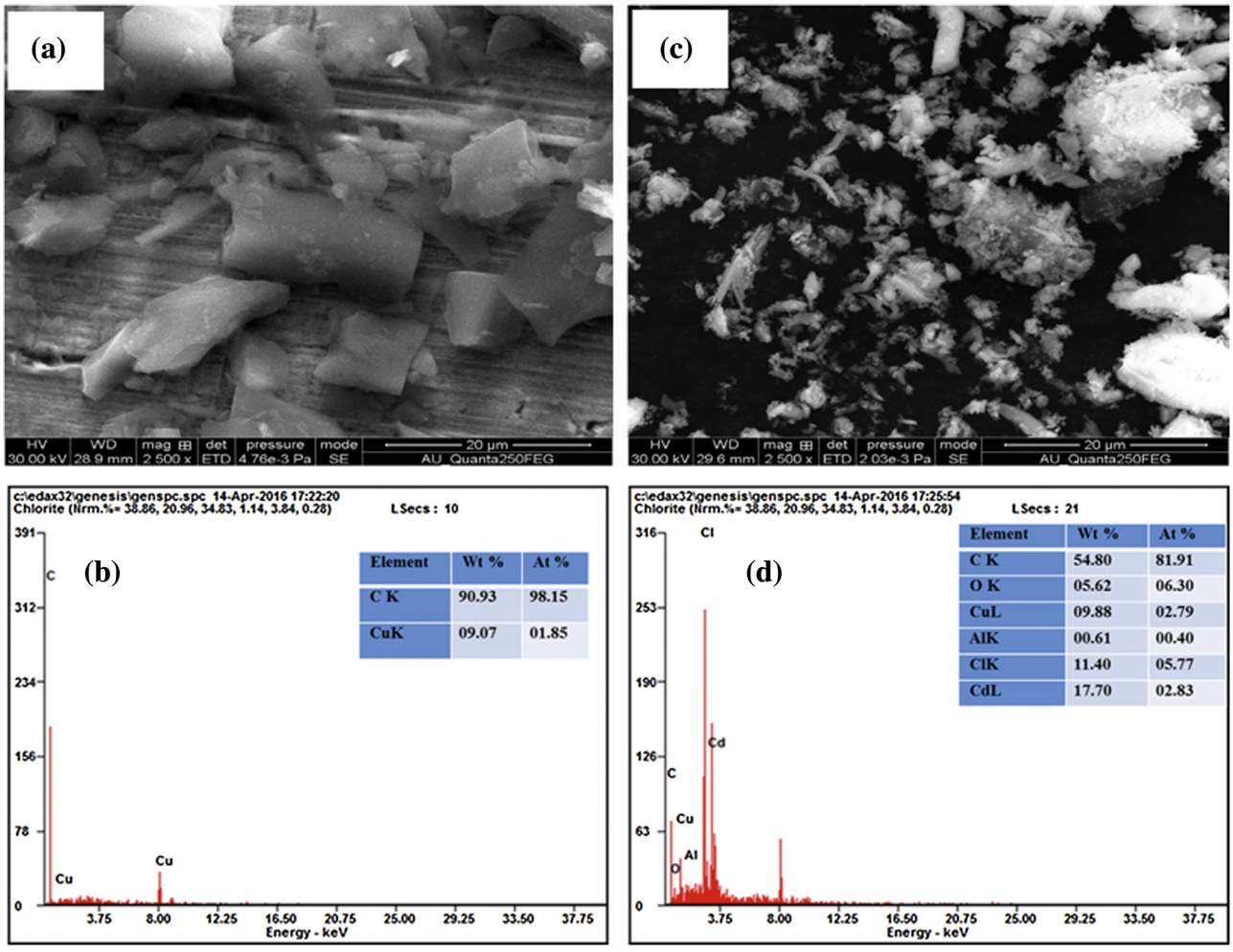

Fig. 12. Scanning electron micrographs of RBD4 and RBD4–Cd^{2+} complex.

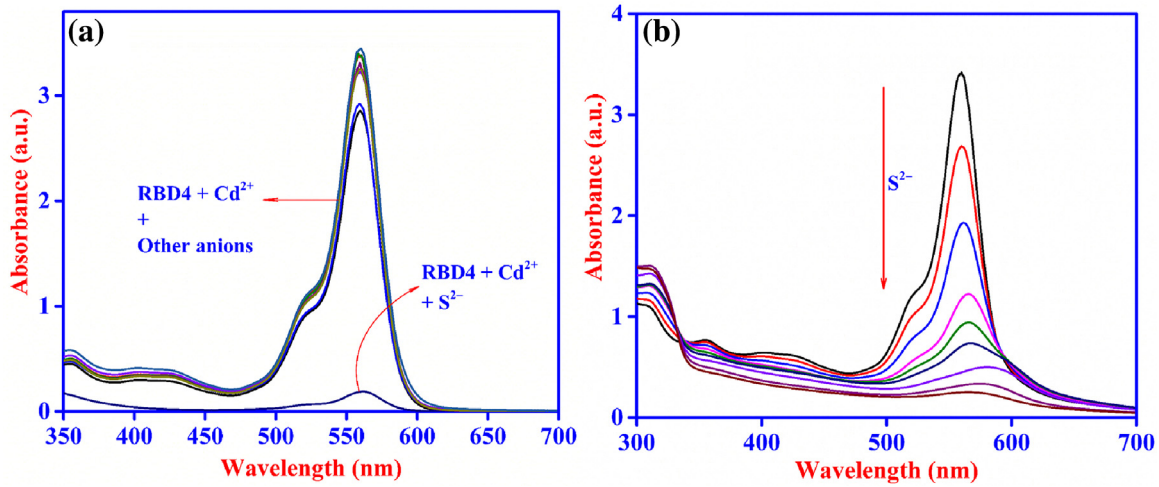

Fig. 13. Changes in the absorption spectra of RBD4–Cd^{2+} complex in presence of different anions (a). UV–vis titration spectra of RBD4 (10 μM) with 5 equiv of Cd^{2+} upon addition of sodium sulfide (30 μM) in ACN/HEPES buffer (2:8, v/v, 10 mM, pH 7.2) (b).

monitoring system is virtually real-time and stable, and the sensor RBD4 was recycled during the detection of sulfide anions. For further investigation, three alternate cycles of titration of RBD4-Cd^{2+} were carried out by introducing S^{2-} into the system (Fig. S10). This results in quenching of fluorescence due to the formation of a CdS_2 complex and thus acts as an OFF switch. However, titration of the receptors with Cd^{2+} resulted in RBD4-Cd^{2+} complex formation, which is accompanied by significant increase in the fluorescence intensities, thereby acting as an ON switch. The high degree of reversibility of the complexation/decomplexation process of the receptors with Cd^{2+} can be achieved several times without a loss of sensitivity of the fluorescence intensity. The comparison of differ-

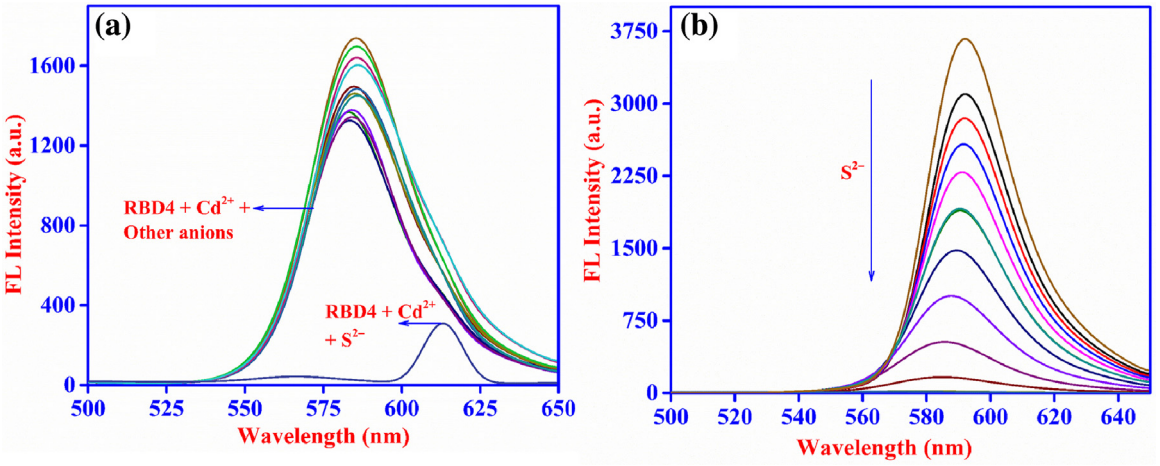

Fig. 14. Changes in the fluorescence spectra of RBD4–Cd^{2+} complex in presence of different anions (a). Fluorescence titration spectra of RBD4 (20 μM) with 5 equiv of Cd^{2+} upon addition of sodium sulfide (30 μM) in aqueous ACN/HEPES buffer (2:8, v/v, 10 mM, pH 7.2) (b).

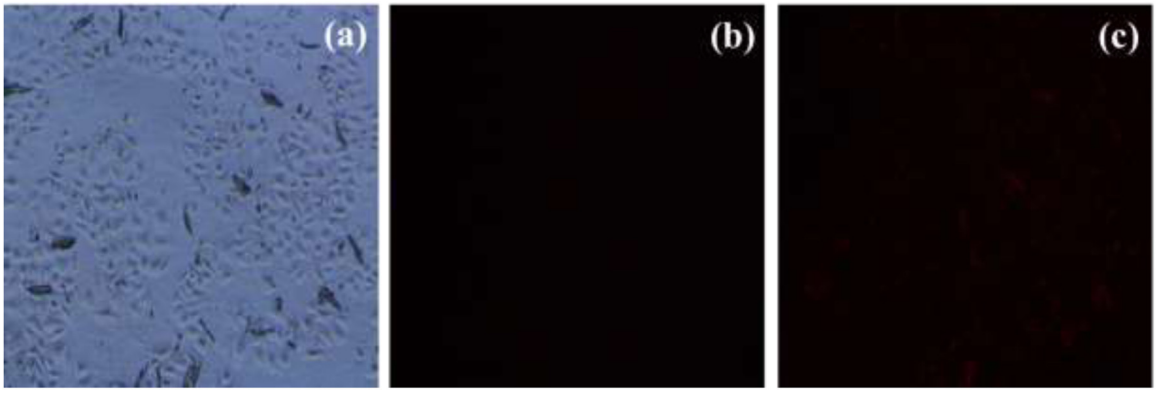

Fig. 15. The fluorescence microscope images of HeLa cells with RBD4–Cd^{2+} (c) showed intense red fluorescence and did not show any fluorescence in the absence of metal ions, probe RBD4 (a), Cd^{2+} (b).

ent fluorescence probes for fluorescent sensing of Cd^{2+} is given in Table S3.

3.10. Bioimaging study

To study the potential use of the fluorescent probe RBD4 in bioimaging applications, we tested the cytotoxicity of RBD4 toward HeLa cells, by the reduction activity of MTT assay (Fig. S11). The viability of untreated cells was assumed to be 100%. Upon incubation of 0–100 μM RBD4 for 12 h, no significant difference in the proliferation of the cells was observed. Especially, cell viabilities of about 80% even at a high-dose concentration of 100 μM Cd^{2+} were observed after 12 h. These data indicated the satisfactory biocompatibility of the Cd^{2+} fluorescent probe at all dosages, thus enabling the RBD4 to serve as a potential probe for fluorescence bioimaging.

In order to develop the application of RBD4 in more complex metrics, we examined the imaging characteristics of RBD4 to cultured living cells in vitro (HeLa, human cervical cancer cell) by fluorescence microscopy (Fig. 15). The cells were incubated with 20 μM RBD4 for 8 h at 37.0 °C. Then the cells were washed with (phosphate-buffered saline) PBS for three times and mounted on a microscope stage. As shown in Fig. 15a and b the cells shows modest intracellular staining after incubation with RBD4, Cd^{2+} for 8 h, indicating that RBD4 was readily taken up by the cells. Upon incubation with 20 μM Cd^{2+} for 8 h, a striking turn-on fluorescence is observed inside HeLa cells, indicating the formation of the RBD4–Cd^{2+} complex (Fig. 15c), aforesaid results conformed to the studies observed in solution. Essentially, the fluorescence microscopic analysis strongly proposed that the probe RBD4 could readily cross the membrane barrier, penetrate into HeLa cells, and rapidly sense intracellular Cd^{2+}.

4. Conclusion

In summary, we have developed a novel turn-on fluorescent chemosensor based on a rhodamine–2-Pyridinecarboxaldehyde conjugate. The sensor RBD4 displays an excellent selectivity and high sensitivity toward the detection of Cd^{2+} in ACN/HEPES buffer (2:8, v/v, pH 7.2, 10 mM) over a wide range of tested metal ions with remarkably enhanced fluorescent intensity and also shows a clear color change from colorless to deep magenta. A comparison of the present probe with other existing Cd^{2+} sensitive "turn-on" fluorescent probes reveals that it is very competitive and somewhat better than others in respect of all the parameters. The present probe RBD4 is relatively cheap as it involves a facile two step reaction with the commercially available much cheaper chemicals. Under UV light illumination, one can visually detect even 1.025×10^{-8} M Cd^{2+} in aqueous–acetonitrile buffer solution using this sensor without the aid of any sophisticated instruments. Thus the chemosensor RBD4 is able to serve as a 'naked eye' chemosensor for Cd^{2+} ions. We believe that RBD4 can be used for many practical applications in chemical, environmental and biological systems.

Conflict of interest

The authors declare that there is no competing financial interest.

Acknowledgments

T. Stalin is grateful to the Department of Science & Technology (DST) India, under the scheme of SERCH FAST Track scheme [No: SR/FT/CS-101/2010 (G)] carringout this work. The authors should thank to the Department of Physics, Alagappa University, providing the XRD and J.Jeyakanthan thanks to DBT and DST for supporting the computational facility. RM thanks to UGC-MANF (F1-17.1/2013-14/MANF-2013-14-CHR-PON-24811) for providing fellowship.

Appendix A. Supplementary data

Supplementary data associated with this article can be found, in the online version, at http://dx.doi.org/10.1016/j.snb.2016.07.102.

References

[1] P. Zhuang, M. McBride, H. Xia, N. Li, Z. Li, Health risk from heavy metals via consumption of food crops in the vicinity of Dabaoshan mine, South China, Sci. Total Environ. 407 (2009) 1551.
[2] M.D. Taylor, Accumulation of cadmium derived from fertilisers in New Zealand soils, Sci. Total Environ. 208 (1997) 123.
[3] L. Järup, M. Berglund, C.G. Elinder, G. Nordberg, M. Vahter, L. Teppo, Health effects of cadmium exposure – a review of the literature and a risk estimate, Scand. J. Work Environ. Health 24 (1998) 1.
[4] A.M.S. Mendes, G.P. Duda, C.W.A. do Nascimento, M.O. Silva, Bioavailability of cadmium and lead in a soil amended with phosphorus fertilizers, Sci. Agricola 63 (2006) 328.
[5] Agency for Toxic Substances and Disease Registry, Atlanta, GA. Online http://www.atsdr.cdc.gov/cercla/07.
[6] L. Friberg, C.G. Elinger, T. Kjellström, Cadmium, World Health Organization, Geneva, Switzerland, 1992.
[7] H. Wang, L. Xue, H. Jiang, Ratiometric fluorescent sensor for silver ion and its resultant complex for iodide anion in aqueous solution, Org. Lett. 13 (2011) 3844.
[8] P.N. Basa, A. Bhowmick, M.M. Schulz, A.G. Sykes, Site-selective imination of an anthracenone sensor: selective fluorescence detection of barium(II), J. Org. Chem. 76 (2011) 7866.
[9] A.E. Palmer, Expanding the repertoire of fluorescent calcium sensors, ACS Chem. Biol. 3 (2009) 157.
[10] J.H. Lee, A.R. Jeong, I.S. Shin, H.J. Kim, J.I. Hong, Fluorescence turn-on sensor for cyanide based on a cobalt(II)-coumarinylsalen complex, Org. Lett. 12 (2010) 764.
[11] M. Zheng, Z. Xie, D. Qu, D. Li, P. Du, X. Jing, Z. Sun, On-off-on fluorescent carbon dot nanosensor for recognition of chromium(VI) and ascorbic acid based on the inner filter effect, ACS Appl. Mater. Interfaces 5 (2013) 13242.
[12] R.E. Clement, P.W. Yang, C. Koester, Environmental analysis, J. Anal. Chem. 71 (1999) 257.
[13] L.H. Thaller, A.H. Zimmerman, Electrolyte management considerations in modern nickel/hydrogen and nickel/cadmium cell and battery designs, J. Power Sources 63 (1996) 53.
[14] S.E. Bailey, T.J. Olin, R.M. Bricka, D.D. Adrian, A review of potentially low costs sorbents for heavy metals, Water Res. 33 (1999) 2469.
[15] M.P. Waalkes, Cadmium carcinogenesis in review, J. Inorg. Biochem. 79 (2000) 241.
[16] M.P. Waalkes, T.P. Coogan, R.A. Barter, Oxicological principles of metal carcinogenesis with special emphasis on cadmium, Crit. Rev. Toxicol. 22 (1992) 175.
[17] H.N. Kim, W.X. Ren, J.S. Kim, J. Yoon, Fluorescent and colorimetric sensors for detection of lead, cadmium, and mercury ions, Chem. Soc. Rev. 8 (2012) 3210.
[18] A.P. de Silva, H.Q.N. Gunaratne, T. Gunnlaugsson, A.J.M. Huxley, C.P. McCoy, J.T. Rademacher, T.E. Rice, Signaling recognition events with fluorescent sensors and switches, Chem. Rev. 97 (1997) 1515.
[19] S.C. Burdette, S.J. Lippard, ICCC34-golden edition of coordination chemistry reviews. Coordination chemistry for the neurosciences, Coord. Chem. Rev. 216–217 (2001) 333.
[20] Y. Ding, W. Zhu, Y. Xu, X. Qian, A small molecular fluorescent sensor functionalized silica microsphere for detection and removal of mercury cadmium, and lead ions in aqueous solutions, Sens. Actuators B 220 (2015) 762–771.
[21] A. Sil, A. Maity, D. Giri, S.K. Patra, A phenylene-vinylene terpyridine conjugate fluorescent probe for distinguishing Cd^{2+} from Zn^{2+} with high sensitivity and selectivity, Sens. Actuators B 226 (2016) 403–411.
[22] D. Liu, J. Qi, X. Liu, Z. Cui, H. Chang, J. Chen, G. Yang, 4-Amino-1,8-naphthalimide-based fluorescent Cd^{2+} sensor with high selectivity against Zn^{2+} and its imaging in living cells, Sens. Actuators B 204 (2014) 655–658.
[23] P.G. Mahajan, D.P. Bhopate, G.B. Kolekar, S.R. Patil, *N*-methyl isatin nanoparticles as a novel probe for selective detection of Cd^{2+} ion in aqueous medium based on chelation enhanced fluorescence and application to environmental sample, Sens. Actuators B 220 (2015) 864–872.
[24] P.D. Beer, P.A. Gale, Anion recognition and sensing: the state of the art and future perspectives, Angew. Chem. Int. Ed. 40 (2001) 486–516.
[25] R. Martínez-Maín˜ez, F. Sancenoín, Fluorogenic and chromogenic chemosensors and reagents for anions, Chem. Rev. 103 (2003) 4419–4476.
[26] Hydrogen Sulfide, World Health Organization, Geneva, 1981 (Environmental Health Criteria, No. 19).
[27] R.E. Gosselin, R.P. Smith, H.C. Hodge, Hydrogen sulfide, in: Clinical Toxicology of Commercial Products, 5th ed., Williams and Wilkins, Baltimore, MD, 1984, pp. III-198–III-202.
[28] S.A. Patwardhan, S.M. Abhyankar, Toxic and hazardous gases, Colourage 35 (1988) 15–18.
[29] P.A. Patnaik, Comprehensive Guide to the Hazardous Properties of Chemical Substances, 3th ed., Wiley, New York, 2007.
[30] J. Fan, M. Hu, P. Zhan, X. Peng, Energy transfer cassettes based on organic fluorophores: construction and applications in ratiometric sensing, Chem. Soc. Rev. 42 (2013) 29.
[31] L. Yuan, W. Lin, K. Zheng, S. Zhu, FRET-based small-molecule fluorescent probes: rational design and bioimaging applications, Acc. Chem. Res. 46 (2013) 1462.
[32] G. Sivaraman, T. Anand, D. Chellappa, Turn-on fluorescent chemosensor for Zn(II) via ring opening of rhodamine spirolactam and their live cell imaging, Analyst 137 (2012) 5881.
[33] G. Sivaraman, V. Sathiyaraja, D. Chellappa, Turn-on fluorogenic and chromogenic detection of Fe(III) and its application in living cell imaging, J. Lumin. 145 (2014) 480–485.
[34] G. Sivaraman, B. Vidya, D. Chellappa, Rhodamine based selective turn-on sensing of picric acid, RSC Adv. 4 (2014) 30828.
[35] G. Sivaraman, T. Anand, D. Chellappa, A fluorescence switch for the detection of nitric oxide and histidine and its application in live cell imaging, ChemPlusChem 79 (2014) 1761.
[36] G. Sivaraman, D. Chellappa, Rhodamine based sensor for naked-eye detection and live cell imaging of fluoride ions, J. Mater. Chem. B 1 (2013) 5768.
[37] T. Anand, G. Sivaramana, A. Mahesh, D. Chellappa, Aminoquinoline based highly sensitive fluorescent sensor for lead(II) and aluminum(III) and its application in live cell imaging, Anal. Chim. Acta 853 (2015) 596–601.
[38] O. Sunnapu, N.G. Kotla, B. Maddiboyina, S. Singaravadivel, G. Sivaraman, A rhodamine based "turn-on" fluorescent probe for Pb(II) and live cell imaging, RSC Adv. 6 (2016) 656.
[39] R. Balasaravanan, V. Sadhasivam, G. Sivaraman, A. Siva, Triphenylamino α-cyanovinyl- and cyanoaryl-based fluorophores: solvatochromism: aggregation-induced emission and electrochemical properties, Asian J. Org. Chem. 5 (2016) 399–410.
[40] K.M. Vengaian, C.D. Britto, K. Sekar, G. Sivaraman, S. Singaravadivel, Phenothiazine-diaminomalenonitrile based colorimetric and fluorescence turn-off-on sensing of Hg^{2+} and S^{2-}, Sens. Actuators B 235 (2016) 232.
[41] T. Anand, G. Sivaraman, M. Iniya, A. Siva, D. Chellappa, Aminobenzohydrazide based colorimetric and 'turn-on' fluorescence chemosensor for selective recognition of fluoride, Anal. Chim. Acta 876 (2015) 1–8.
[42] X. Chen, T. Pradhan, F. Wang, J.S. Kim, J. Yoon, Fluorescent chemosensors based on spiroring-opening of xanthenes and related derivatives, Chem. Rev. 112 (2012) 1910.
[43] L. Zhou, X. Zhang, Q. Wang, Y. Lv, G. Mao, A. Luo, Y. Wu, Y. Wu, J. Zhang, W. Tan, Molecular engineering of a TBET-based two-photon fluorescent probe for ratiometric imaging of living cells and tissues, J. Am. Chem. Soc. 136 (2014) 9838.
[44] S. Sun, B. Qiao, N. Jiang, J. Wang, S. Zhang, X. Peng, Naphthylamine-rhodamine-based ratiometric fluorescent probe for the determination of Pd^{2+} ions, Org. Lett. 16 (2014) 1132.
[45] X. Zhou, X. Wu, J. Yoon, A dual FRET based fluorescent probe as a multiple logic system, Chem. Commun. 51 (2015) 111.
[46] F. Hu, B. Zheng, D. Wang, M. Liu, J. Du, D. Xiao, A novel dual-switch fluorescent probe for Cr(III) ion based on PET-FRET processes, Analyst 139 (2014) 3607.
[47] W.-D. Chen, W.-T. Gong, Z.-Q. Ye, Y. Lin, G.-L. Ning, FRET-based ratiometric fluorescent probes for selective Fe3+ sensing and their applications in mitochondria, Dalton Trans. 42 (2013) 10093.
[48] W. Xuan, Y. Cao, J. Zhou, W. Wang, A FRET-based ratiometric fluorescent and colorimetric probe for the facile detection of organophosphonate nerve agent mimic DCP, Chem. Commun. 49 (2013) 10474.
[49] M. Shanmugam, D. Ramesh, V. Nagalakshmi, R. Kavitha, R. Rajamohan, T. Stalin, Host-guest interaction of L-tyrosine with beta-cyclodextrin, Spectrochim. Acta Part A 71 (2008) 125–132.
[50] K. Srinivasan, K. Kayalvizhi, K. Sivakumar, T. Stalin, Study of inclusion complex of β-cyclodextrin and diphenylamine: photophysical and electrochemical behaviors, Spectrochim. Acta Part A 79 (2011) 169–178.
[51] K. Srinivasan, T. Stalin, K. Sivakumar, Spectral and electrochemical study of host-guest inclusion complex between 2,4-dinitrophenol and β-cyclodextrin, Spectrochim. Acta Part A 94 (2012) 89–100.
[52] K. Srinivasan, T. Stalin, Study of inclusion complex between 2,6-dinitrobenzoic acid and β-cyclodextrin by ^{1}H NMR, 2D ^{1}H NMR (ROESY), FT-IR, XRD, SEM and photophysical methods, Spectrochim. Acta Part A 130 (2014) 105–115.

[53] K. Srinivasana, S. Radhakrishnan, T. Stalin, Inclusion complexes of β-cyclodextrin-dinitrocompounds as UV absorber for ballpoint pen ink, Spectrochim. Acta Part A 129 (2014) 551–564.
[54] S. Mohandoss, M. Maniyazagan, T. Stalin, A highly selective dual mode detection of Fe^{3+} ion sensing based on 1: 5-dihydroxyanthraquinone in the presence of β-cyclodextrin, Mater. Sci. Eng. C 48 (2015) 94–102.
[55] S. Mohandoss, J. Sivakamavalli, B. Vaseeharan, T. Stalin, Fluorometric sensing of Pb^{2+} and $CrO_4^{2?}$ ions through host–guest inclusion for human lung cancer live cell imaging, RSC Adv. 5 (2015) 101802–101818.
[56] M. Maniyazagan, S. Mohandoss, K. Sivakumar, T. Stalin, *N*-phenyl-1-naphthylamine/β-cyclodextrin inclusion complex as a new fluorescent probe for rapid and visual detection of Pd^{2+}, Spectrochim. Acta Part A 133 (2014) 73–79.
[57] W. Koch, M.C. Holthausen, A Chemist's Guide to Density Functional Theory, Wiley-VCH, Weinheim, 2000.
[58] A.D. Becke, Density-functional thermochemistry. III. The role of exact exchange, J. Chem. Phys. 98 (1993) 5648.
[59] C. Lee, W. Yang, R.G. Parr, Development of the Colle-Salvetti correlation-energy formula into a functional of the electron density, Phys. Rev. B 37 (1988) 785.
[60] A.D. Becke, Density-functional exchange-energy approximation with correct asymptotic behavior, Phys. Rev. A: Atom. Mol. Opt. Phys. 38 (1988) 3098.
[61] Y. Xiang, A. Tong, P. Jin, Y. Ju, New fluorescent rhodamine hydrazone chemosensor for Cu(II) with high selectivity and sensitivity, Org. Lett. 8 (2006) 2863.
[62] K.A. Connors, Binding Constants, Wiley, New York, 1987.
[63] W.C. Vosburgh, G.R. Copper, Complex ions. I. The identification of complex ions in solution by spectrophotometric measurements, J. Am. Chem. Soc. 63 (1941) 437.
[64] G.L. Long, J.D. Winefordner, Limit of detection. A closer look at the IUPAC definition, Anal. Chem. 55 (1983) 712A.

Biographies

M. Maniyazagan received his M.Sc. degree in organic chemistry from Muthayammal college of Arts and Science, Periyar University, India in 2008. He is currently a Ph.D. candidate working in synthesis of rhodamine based derivatives and fluorescent sensor materials under the guidance of Dr. T. Stalin at Department of Industrial Chemistry, Alagappa University, Karaikudi, India.

R. Mariadasse received his M.Sc. degree from Pondicherry University in 2013. Currently he is working as a Ph.D. Research Scholar under the guidance of Dr. J. Jeyakanthan at Department of Bioinformatics, Alagappa University, Karaikudi, Tamil Nadu, India. His research interests focus on the Computer Aided Drug Design.

P. Muthuraja has obtained his Master Degree in Chemistry in 2008 and now is pursuing for his Doctoral degree under the guidance of Dr. P. Manisankar at Department of Industrial Chemistry, Alagappa University, Karaikudi, India.

Dr. S. Naveen obtained MSc and PhD in Physics from the University of Mysore, Mysore. Presently he is working as a Scientist at The Institution of Excellence, University of Mysore, India. He was a Centenary Postdoctoral fellow at the Molecular Biophysics Unit, Indian Institute of Science, Bangalore. Dr. Naveen has published more than 150 articles in International journals of high repute and is a member of many professional bodies.

Dr. N. K. Lokanath obtained PhD in Physics from the University of Mysore, Mysore. Presently he is working as a Professor at Dept. of Studies in Physics, University of Mysore, India. Recently, he was awarded the Sir C V. Raman Young Scientist's State Award from Government of Karnataka for his outstanding contribution towards science. Prof. Lokanath's area of research includes structural biology and new materials. He solved the first crystal structure of A-ATPase from *Pyrococcus horikoshii* which was acclaimed worldwide as a significant finding. He has determined structures of more than 75 proteins and has published more than 150 articles.

Dr. J. Jeyakanthan, Professor and Head in the Department of Bioinformatics, Alagappa University, Karaikudi. He has published 83 research articles in the reputed National and International journals and more than 100 Protein crystal structures depositions in Protein Data Bank (PDB). He has received Rs. 2.21 cores funds from various agencies such as UGC, DBT, and DST and being the Coordinator of UGC Sponsored Innovative Scheme in the department. He is visiting scientist of Osaka University and RIKEN Spring-8 Institute, Japan. Currently, 8 scholars are doing Ph.D under his guidance. He has visited many countries.

K. Premkumar Assistant Professor in Biomedical Science at Bharathidasan University, India. He received Ph.D (Genetics) from Department of Genetics, Dr. ALM Postgraduate Institute of Basic Medical Sciences, University of Madras. He was a Post-Doctoral Researcher and Research Associate at Department of Internal Medicine, University of California and Center for Pharmacogenetics, University of Pittsburgh. He has authored and co-authored around 50 peer reviewed articles in highly reputed journals. He is a recipient of DST-Young Scientist Award, INSA Visiting Fellowship Award and UGC Raman Fellowship from the Govt. of India. His research interests include Cancer biology Genomic Instability and Nanomedicine.

Dr. P. Manisankar is currently Professor and Head, Department of Industrial Chemistry, Alagappa University, Karaikudi, Tamil Nadu, India. He obtained his M.Sc. from V.O.C. College, Tuticorin and Ph.D. from Madurai Kamaraj University, Madurai. His current research area of interest include conducting polymer composites, sensors, dye sensitized solar cells, green synthesis of organic compounds. He has generated funds to the tune of Rs.400 lakhs. He is a receipient of TANSA 2009 award from Tamil Nadu State Council for Science and Technology and UGC BSR one time grant award. He has produced 30 Ph.D scholars published 172 papers in the referred journals.

T. Stalin is an Assistant Professor of Chemistry in the Department of Industrial Chemistry at Alagappa University, Tamilnadu, India. He received his Ph.D., degree from the Annamalai University, India in 2008. He is recipient of Department of Science and Technology (DST INDIA) Fast Track Young Scientist Award and also he received prestigious award of UGC Raman Fellowship for Post-Doctoral Research for Indian Scholars in United States of America (2015–2016 batch). He is a Life member of the Indian science congress Association, Solid State Chemistry. His Current research interest involves the development of chemosensor materials for environmental and biological applications.